

Second-nearest-neighbor modified embedded-atom potential for binary Ta-W alloys based on first-principles calculations

C. Bercegeay, G. Jomard, and S. Bernard

Département de physique théorique et appliquée, CEA/DAM Ile-de-France, BP 12, 91680 Bruyères-le-Châtel, France

(Received 4 September 2007; revised manuscript received 13 December 2007; published 10 March 2008)

We present a methodology to construct a Ta-W cross potential for Ta-W binary alloys, in the second nearest-neighbor modified embedded atom method formalism, based on *ab initio* calculations. The first attempt has consisted in fitting the potential on a single reference structure, and has led to a poorly transferable potential, particularly in the W-poor region. Improving our procedure of parametrization by taking into account various structures to fix the angular screening parameters, we have been able to obtain a more transferable potential. The formation energies of some structures not used in the adjustment of the potential and energies of body-centered cubic solid solutions reproduce experimental tendencies. We have also tested the ability of our improved potential to predict melting temperatures of Ta-W alloys.

DOI: [10.1103/PhysRevB.77.104203](https://doi.org/10.1103/PhysRevB.77.104203)

PACS number(s): 61.82.Bg, 64.70.D-, 61.43.Bn, 61.50.Lt

I. INTRODUCTION

Thermodynamic properties of alloys (and especially very dilute alloys) are still beyond the reach of fully *ab initio* calculations, as they may require very big simulation cells and long simulation times, in order to equilibrate the system to the required temperatures and pressures. In order to overcome these limitations, one can build an effective medium which will account for the chemical randomness of the alloy state (see, for example, Refs. 1 and 2). Another possibility is to perform large scale classical molecular dynamics (MD) simulations.

We have chosen here this second approach. In this case, the first step is to build effective interaction potentials for the system.

More or less sophisticated types of effective potentials for pure metals have been developed in the literature. It is more challenging to build a cross potential, which will guarantee a good transferability, in other terms a good prediction of thermodynamic quantities, whatever the proportions of each component in the alloy.

We will focus here on binary Ta-W substitutional alloys, because various theoretical data exist in the literature,¹⁻³ and all compounds—pure metals, definite compounds and alloys—have the same crystallographic structure: A body centered structure.

Our main interest in this paper is in the methodology to build a cross potential from first-principles calculations. However, we will present a first application to the prediction of the melting properties of these compounds by large scale phase-coexistence MD simulations.

The second nearest-neighbor modified embedded atom method (2NN-MEAM) formalism is now widely used to treat bcc transition metals. Potentials in this formalism for pure Ta and W have been previously published.⁴ We thus have decided to work within this formalism.

The paper is organized as follows. Section II will be dedicated to the *ab initio* calculations whose results were used as input data for the semiempirical potentials. In Sec. III the methodology to construct the cross potential will be presented and the transferability of such a potential will be

tested. In Sec. IV we will briefly detail the phase-coexistence MD method we used here and we will report the melting temperatures predicted for binary Ta-W alloys.

II. *Ab initio* CALCULATIONS

According to the assessed phase diagram of the Ta-W system, Ta and W form a continuous series of bcc solid solutions. No existence of intermediate phases has been found. Experimental data have been reported in the literature^{5,6} and different theoretical studies have been done on Ta-W alloys.¹⁻³ The first-principles study of Turchi *et al.*¹ within the tight-binding linear muffin-tin orbital (TB-LMTO) formulation of the coherent potential approximation (CPA) led to the prediction of two ordered phases: *B2* (TaW) and *DO₃* (TaW₃ and Ta₃W). Jiang *et al.*² performed *ab initio* calculations using a plane wave method with Vanderbilt ultrasoft pseudopotentials (US-PP) and the generalized gradient approximation (GGA). They used 16-atom special quasirandom structures (SQS) to represent Ta_{1-x}W_x random bcc alloys. The predicted equilibrium lattice parameters show a negative deviation from Vegard's law as experiment does. Both the plane wave method with US pseudopotentials and TB-LMTO CPA approach exhibit formation enthalpies with a strong asymmetry towards the W-rich side, whereas experimental measurements of Singhal and Worrell⁶ show a strong asymmetry towards the Ta-rich side. Both Jiang *et al.* and Turchi *et al.* pointed out that such discrepancies between prediction and experiment may be attributed to the slow kinetics at the experimental temperature of 1200 K where thermodynamic equilibrium is difficult to reach. Blum *et al.* have recently applied the mixed-basis cluster expansion (MBCE) approach³ to the Ta-W system. They found that the *C11_b* structure is more stable than the ground states *B2* and *DO₃* predicted by Turchi *et al.* The ground state at equiatomic composition is closely related to the *B2* structure and is labeled *B2₃* (see Fig. 3 of Ref. 3). In the moderately W-rich side the dominant ground states are superlattices *C11_b* and “*Mo₃Ta₂*,” whereas in the moderately Ta-rich side, much more complex structures are found: “*Mo₄Ta₉*,” and “*Mo₄Ta₁₂*.” Additional information about Mo-Ta type structures can be found in Refs. 7 and 8.

TABLE I. Equilibrium lattice parameters and formation energies of Ta-W alloys obtained from our first-principles calculations. The Ta_3W_2 compound was constructed by substituting Ta atoms to Mo atoms and vice versa, by then replacing Mo atoms by W atoms, in the “ Mo_3Ta_2 ” structure.

Structure	x_W	a_0 (Å)	E^f (mRy/atom)
Ta (bcc)	0.00	3.321	
Ta ₁₅ W	0.06	3.310	-0.69
Ta ₃ W (DO_3)	0.25	3.281	-3.21
Ta ₃ W (SQS-16)	0.25	3.280	-3.15
Ta ₁₂ W ₄ (“ $\text{Mo}_4\text{Ta}_{12}$ ”)	0.25	3.275	-4.94
Ta ₉ W ₄ (“ Mo_4Ta_9 ”)	0.31	3.272	-3.21
Ta ₂ W ($C11_b$)	0.33	3.259	-5.87
Ta ₃ W ₂ (“ Mo_3Ta_2 ”)	0.40	3.261	-6.45
TaW ($B2$)	0.50	3.245	-7.61
TaW (SQS-16)	0.50	3.245	-5.70
TaW ($B32$)	0.50	3.244	-5.46
Ta ₃ W ₄	0.57	3.255	-6.51
Ta ₂ W ₃ (“ Mo_3Ta_2 ”)	0.60	3.232	-8.98
TaW ₂ ($C11_b$)	0.67	3.220	-8.58
TaW ₃ (DO_3)	0.75	3.215	-6.71
TaW ₃ (SQS-16)	0.75	3.217	-5.79
TaW ₅ (AB_5)	0.83	3.208	-5.26
TaW ₁₅	0.94	3.196	-2.26
W (bcc)	1.00	3.190	

Our first-principles calculations were performed in the framework of the density functional theory (DFT),⁹ by using the projector augmented wave (PAW) method, as implemented in Vienna Ab initio Simulation Package (VASP).¹⁰ The exchange-correlation functional was GGA as parametrized by Perdew and Wang (PW91).¹¹ Integration over the Brillouin zone was done using the special \mathbf{k} -point scheme of Monkhorst and Pack,¹² the \mathbf{k} -point sets were generated automatically. Their number vary for each structure, but we used typically 56 \mathbf{k} points for the $B32$ structure and 144 \mathbf{k} points for the “ Mo_3Ta_2 ” one, in the irreducible Brillouin zone. The electronic levels were populated according to the Methfessel and Paxton scheme.¹³ The calculations were done at the equilibrium volume with all atomic positions relaxed. The energy cutoff for the plane waves expansion of the wave functions was 600 eV. Spin-orbit coupling was not taken into account in our first-principles calculations. Our previous calculations on pure Ta and W, which are detailed elsewhere¹⁴ showed that it only led to relative variations of 0.2% and 1% on respectively equilibrium volumes and bulk moduli. The cutoff energy, the number of \mathbf{k} points, and the smearing for the Brillouin zone integration were determined by performing energy convergence tests for tantalum, tungsten, and Ta-W alloys, in order to obtain total energies converged to 1 mRy per atom.

Formation energies are defined as

$$E_{A_{1-x}B_x}^f = E_{A_{1-x}B_x}^{\text{eq}} - [(1-x)E_A^{\text{eq}} + xE_B^{\text{eq}}], \quad (1)$$

where x is the composition of B element. E^{eq} are the energies at 0 K for pure metals A and B and their alloys $A_{1-x}B_x$. We

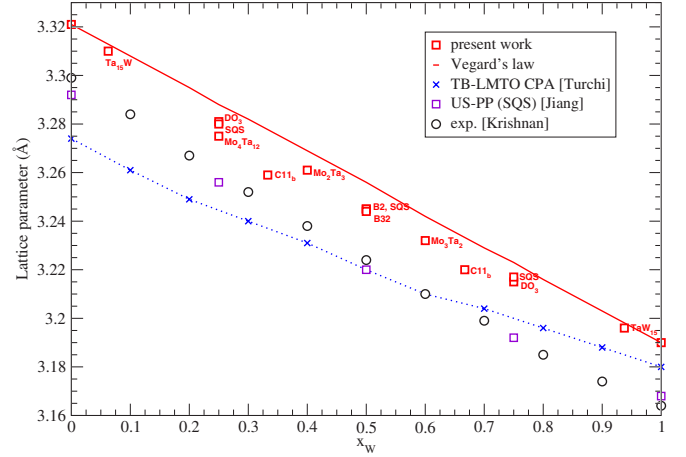


FIG. 1. (Color online) Equilibrium lattice parameters of Ta-W alloys as a function of W composition, as obtained from our work, previous first-principles calculations (Refs. 1 and 2) and experimental data (Ref. 5).

calculated the formation energies of several structures: $B2$, DO_3 , 16-atom SQS for compositions 0.25, 0.50, and 0.75², two 16-atom supercells Ta_{15}W and TaW_{15} with one atom of different type located at position $(\frac{1}{2}, \frac{1}{2}, \frac{1}{2})$, $C11_b$, $B32$ and “ $\text{Mo}_{1-x}\text{Ta}_x$ ” type.³ Some were dedicated to the adjustment of the MEAM potential, whereas others were specifically used to test the transferability of this potential. This will be detailed in Sec. III. Our *ab initio* results are reported in Table I.

They confirm the tendencies already found in previous DFT calculations for these compounds. As we can see on Fig. 1 our first-principles lattice parameters for Ta-W alloys exhibit a negative departure from Vegard’s law, given by

$$\delta a^{\text{eq}} = a_{\text{alloy}}^{\text{eq}} - x a_W^{\text{eq}} - (1-x) a_{\text{Ta}}^{\text{eq}}. \quad (2)$$

In Figs. 1 and 2, the SQS structures of Jiang *et al.*² are in slightly better agreement to experiment than ours (which overestimate it by less than 1%). Actually, Jiang *et al.* used ultrasoft pseudopotentials which give better lattice constants

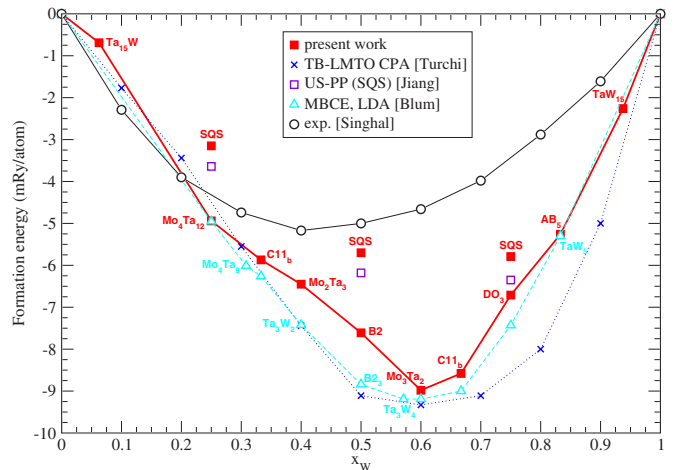
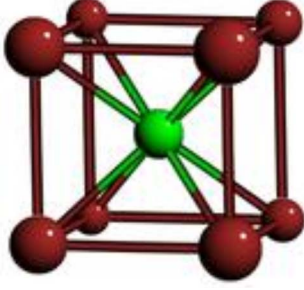


FIG. 2. (Color online) Formation energies of Ta-W alloys as a function of W composition, as obtained from our work, previous theoretical studies (Refs. 1–3) and experiment (Ref. 6).

FIG. 3. (Color online) $B2$ structure.

for the pure metals. However, we decided to keep our PAW potentials, even if they are not perfect, as they enabled us to perform full relaxations of the atomic positions for large cells at a more reasonable computer cost.

On Fig. 2, we can see that experimental formation energies show some asymmetry towards the Ta-rich side, whereas our calculated formation energies exhibit a strong asymmetry towards the W-rich side, as all the other theoretical approaches (either CPA¹ or ultrasoft pseudopotentials²) do.

Let us recall here that the experimental data were obtained at high temperature (1200 K), whereas first-principles data are 0 K data.

In the next section we present the methodology we have adopted to construct a semiempirical potential for a binary alloy, based on these *ab initio* calculations.

III. CONSTRUCTION OF A MEAM POTENTIAL FOR BINARY ALLOYS

Daw and Baskes^{15–17} initially developed EAM potentials for metals by assuming that the cohesive energy of a metal could be accounted for by embedding an atom in the local electron density induced by neighboring atoms. The modified embedded atom method (MEAM) was introduced by Baskes^{18–21} by extending the embedded atom method (EAM), so that the directionality of bonding in the metal is considered. In the original formalism of the MEAM, only interactions between first nearest-neighbor atoms were considered by using a strong screening function. Then the second nearest-neighbor MEAM, labeled 2NN-MEAM, has been developed by Baskes and co-workers^{4,22} in order to solve problems encountered with 1NN-MEAM potentials for bcc metals. The 2NN-MEAM formalism is now routinely applied to all bcc transition metals: Fe, Cr, Mo, W, V, Nb, and Ta.⁴

Details on the 1NN-MEAM and 2NN-MEAM formalisms have been published in the literature respectively in Refs. 18–21 and 23–25 and Refs. 4 and 22. Here we will only give its applications to describe binary alloy systems.

Some parameters of the 2NN-MEAM potentials for pure Ta and W were based on the developed 2NN-MEAM potentials of Lee *et al.*;⁴ the others were fitted on our *ab initio* equations of state.

Let us now turn to the construction of a 2NN-MEAM Ta-W cross potential for the Ta-W system.

We have adopted here the technique proposed by Lee and Baskes *et al.*⁴ First, one has to choose a reference structure for which the analytic expression of the cross potential is written. For convenience, we chose as reference structure a perfectly ordered binary intermetallic compound where one type of atom has only different type of atoms as first nearest-neighbors and has only the same type of atoms as second nearest-neighbors. The $B2$ (CsCl type) ordered structure is a good example. This structure is represented on Fig. 3.

For this particular structure (TaW compound), the total energy per atom is given by

$$E_{\text{TaW}}^u(R) = \frac{1}{2} \left[F_{\text{Ta}}(\bar{\rho}_{\text{Ta}}) + F_{\text{W}}(\bar{\rho}_{\text{W}}) + Z_1^{\text{TaW}} \Phi_{\text{TaW}}(R) + \frac{1}{2} Z_2^{\text{TaW}} \{ S_{\text{Ta}} \Phi_{\text{TaTa}}(aR) + S_{\text{W}} \Phi_{\text{WW}}(aR) \} \right]. \quad (3)$$

Z_1^{TaW} and Z_2^{TaW} are respectively the number of first and second nearest neighbors in the compound. For the $B2$ structure, they are respectively equal to 8 and 6. S_{Ta} and S_{W} represent the angular screening of the second nearest-neighbors interactions, induced by the first nearest-neighbor atoms and first nearest-neighbor distances. F_{Ta} and F_{W} are the embedding functions, Φ_{TaTa} and Φ_{WW} are the 2NN-MEAM potentials for pure Ta and W. As mentioned above, these four terms are already known.⁴ $\bar{\rho}_{\text{Ta}}$ and $\bar{\rho}_{\text{W}}$ are the background electron densities at a Ta site and a W site. In Eq. (3), a is the ratio of the second and first nearest-neighbor distances. For a bcc structure, a is equal to $2/\sqrt{3}$.

An analytical form of the interaction potential Φ_{TaW} can be obtained by inverting Eq. (3):

$$\Phi_{\text{TaW}}(R) = \frac{1}{Z_1^{\text{TaW}}} \left[2E_{\text{TaW}}^u(R) - F_{\text{Ta}}(\bar{\rho}_{\text{Ta}}) - F_{\text{W}}(\bar{\rho}_{\text{W}}) - \frac{1}{2} Z_2^{\text{TaW}} \{ S_{\text{Ta}} \Phi_{\text{TaTa}}(aR) + S_{\text{W}} \Phi_{\text{WW}}(aR) \} \right]. \quad (4)$$

TABLE II. Parameters of the 2NN-MEAM potentials for pure Ta and W. All parameters are from Ref. 4 except those which correspond to the equation of state (E^0 , α , R^0 , K_0 , d). These are obtained from our *ab initio* calculations. Energies are in eV, lattice parameters in Å, and bulk moduli in GPa.

	E^0	R^0	K_0	α	A	$\beta^{(0)}$	$\beta^{(1)}$	$\beta^{(2)}$	$\beta^{(3)}$	$t^{(1)}$	$t^{(2)}$	$t^{(3)}$	C_{max}	C_{min}	S	d
Ta	8.09	2.88	194.0	4.96	0.67	4.49	1.0	1.0	1.0	1.7	2.1	-3.2	2.80	0.25	0.93	0.0
W	8.66	2.76	314.0	5.65	0.40	6.54	1.0	1.0	1.0	-0.6	0.3	-8.7	2.80	0.49	0.89	0.0

TABLE III. Rose equation parameters for the $B2$ structure.

E^0 (eV)	R^0 (Å)	α	d
8.48	2.81	5.28	0.00

As for each of the radial functions, a radial cutoff is applied to the Φ_{TaW} potential, in addition to the angular screening. E_{TaW}^u is the energy per atom of the compound TaW in the $B2$ structure. It is assumed that it can be described by the universal binding energy relation (UBER) of Rose²⁶ to the third order:

$$E_{\text{TaW}}^u(R) = -E_{\text{TaW}}^0(1 + a^* + da^{*3})e^{-a^*} \quad (5)$$

with

$$a^* = \alpha_{\text{TaW}}(R/R_{\text{TaW}}^0 - 1) \quad (6)$$

and

$$\alpha_{\text{TaW}} = \left(\frac{9K_0V_0}{E_{\text{TaW}}^0} \right)^{1/2}. \quad (7)$$

E_{TaW}^0 is the cohesive energy, R_{TaW}^0 is the equilibrium nearest-neighbor distance, K_0 is the bulk modulus, and V_0 is the equilibrium atomic volume. These physical properties can be measured experimentally or calculated by first-principles methods. Here we have chosen to fit the semiempirical potential on our *ab initio* results.

The interaction potential Φ_{TaW} is thus completely defined if we know the equation of state of $B2$ structure at 0 K, which is determined by the four parameters E_{TaW}^0 , α_{TaW} , R_{TaW}^0 , and d . We report in Table II the values of the different parameters for pure Ta and W extracted from Ref. 4, except the four Rose coefficients, which were adjusted on the 0 K equation of state obtained in our first-principles calculations.

A. First fitted potential

The first step of our study was to fit the potential on the cold curve of the $B2$ structure of the TaW compound. The values of the equation of state parameters are presented in Table III. One can notice that we finally chose to use a UBER of Rose to the first order. In fact we found that all our potentials fitted with a third order UBER of Rose were unstable in MD simulations at high temperature.

For example, a potential fitted with $d=0.046$ was eliminated because with such a potential, the $B2$ compound is unstable in MD simulations, in the (NVE) thermodynamical ensemble, for temperatures of the order of 4000 K. It is thus inappropriate for calculating melting temperatures of the Ta-W system.

In a first approximation²⁷ the screening function in Ta-W alloys has been defined by the two following parameters:

$$C_{\text{min}}^{\text{Ta-X-W}} = \left[\frac{1}{2}\sqrt{C_{\text{min}}^{\text{Ta}}} + \frac{1}{2}\sqrt{C_{\text{min}}^{\text{W}}} \right]^2 \quad (8)$$

and

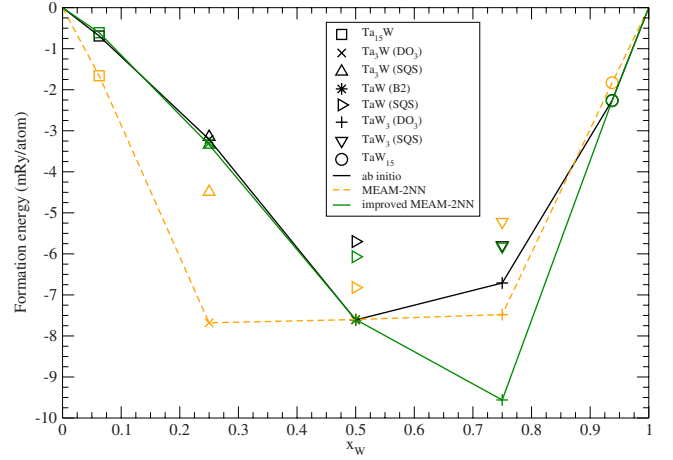


FIG. 4. (Color online) Formation energies obtained by the 2NN-MEAM potential fitted on $B2$ structure and the improved one, compared with our *ab initio* calculations.

$$C_{\text{max}}^{\text{Ta-X-W}} = \left[\frac{1}{2}\sqrt{C_{\text{max}}^{\text{Ta}}} + \frac{1}{2}\sqrt{C_{\text{max}}^{\text{W}}} \right]^2, \quad (9)$$

where atom X is either of Ta or W type. In this case $C_{\text{min}}^{\text{Ta-X-W}}$ and $C_{\text{max}}^{\text{Ta-X-W}}$ are respectively equal to 0.36 and 2.80, whatever type of atom X is.

We have calculated the formation energies of all the compounds studied with DFT, with this first 2NN-MEAM potential. They are reported in Table IV and on Fig. 4. The results are in poor agreement with our *ab initio* calculations except for the structure used for the fit. This potential is thus not transferable, and particularly for the W-poor region; that suggests that our model is too simplified. We will show in the next section how we have improved this potential.

B. Improvement of the first-fitted MEAM potential

To improve the transferability of our potential we decided to take into account more structures by modifying the angular screening, which in the first potential did not depend on the type of the central atom in the interactions Ta-X-Ta, Ta-X-W, and W-X-W, in order to better describe atomic interactions in Ta-W alloys. One way to do that, is to introduce C_{max} and C_{min} screening parameters for all three-atoms interactions encountered in Ta-W alloys. The way we have chosen to optimize the $C_{\text{min,max}}^{ijk}$ parameters is by minimizing an error function which represents the difference between reference *ab initio* data and data calculated with a given set of parameters. We have adopted the following simple form for the error function:

$$\dot{F} = \sum_{i=1}^N p_i \cdot \left| \frac{f_i - f_i^{\text{ref}}}{f_i^{\text{ref}}} \right|, \quad (10)$$

where N is the number of reference data, f_i^{ref} is the reference data, f_i is the calculated data in the MEAM formalism, and p_i the relative weight given to the property i in the error function. In our case we have eight parameters to determine: $C_{\text{min,max}}^{\text{TaW-Ta}}$, $C_{\text{min,max}}^{\text{TaTaW}}$, $C_{\text{min,max}}^{\text{TaWW}}$, and $C_{\text{min,max}}^{\text{WTaW}}$ as the remaining

TABLE IV. Formation energies of $Ta_{1-x}W_x$ intermetallic compounds obtained with the 2NN-MEAM potentials. All atomic positions are relaxed. Formation energies are in mRy/atom; lattice parameters in Å.

Structure	x_W	<i>Ab initio</i>		2NN-MEAM	improved 2NN-MEAM	
		a_0	E^f	E^f	a_0	E^f
Ta ₁₅ W	0.06	3.310	-0.69	-1.66	3.312	-0.61
Ta ₃ W (<i>DO</i> ₃)	0.25	3.281	-3.21	-7.68	3.283	-3.30
Ta ₃ W (SQS-16)	0.25	3.280	-3.15	-4.49	3.284	-3.34
TaW (<i>B2</i>)	0.50	3.245	-7.61	-7.60	3.246	-7.60
TaW (SQS-16)	0.50	3.245	-5.70	-6.82	3.249	-6.07
TaW ₃ (<i>DO</i> ₃)	0.75	3.215	-6.71	-7.48	3.218	-9.56
TaW ₃ (SQS-16)	0.75	3.217	-5.79	-5.22	3.218	-5.82
TaW ₁₅	0.94	3.196	-2.26	-1.83	3.197	-2.27

$C_{\min, \max}^{TaTaTa}$ and $C_{\min, \max}^{WWW}$ are known from the adjustment of the pure metals potentials. In order to span the entire set of $C_{\min, \max}^{ijk}$ parameters, we decided to treat three 16-atoms SQS, two *DO*₃, and two supercells TaW₁₅ and Ta₁₅W, as well as the *B2* structure in our *ab initio* reference data set. The properties entering the error function were the total energies of all these structures. The optimization problem has been solved by using the simple steepest descent routine of Powell with a random exploration of the parameters constrained to lie in the range [0,4]. This procedure uses the pseudorandom number generator proposed by Marsaglia²⁸ which is based on the Box-Muller algorithm.²⁹ Among the hundreds of optimization performed, the best error function found was of the order of 10^{-2} . The corresponding obtained parameters are given in Table V. We will see in the following section, that the transferability of the so-obtained cross potential is greatly improved compared to the one of our first fitted potential.

Note that we have tested another approach to improve the transferability of our potential by introducing a dependance on the chemical environment in the density weights $t^{(l)}$, as suggested by Ni *et al.*³⁰ It appears that this technique can only be used to perform calculations with fixed atomic positions. When we tried to do molecular dynamics simulations, we faced insoluble problems of instabilities.

C. Transferability of the fitted potential

In order to test the transferability of our improved cross potential, we have calculated formation energies of $Ta_{1-x}W_x$ compounds which have not been included in the parametrization procedure. We have also generated bcc solid solutions at 0 K. These results are compared with experimental data^{5,6} and *ab initio* calculations¹⁻³ when available. The corresponding values are listed in Table VI for intermetallic compounds

and in Table VII for solid solutions. These results are also reported on Figs. 5 and 6. We can see that the overall agreement is much better, even if not perfect for the TaW₃ structure.

We find that, at 0 K, the intermetallic compounds are more stable than both the special quasirandom structures and the solid solutions. However, we know experimentally that, at least at high temperatures (1200 K), Ta and W form continuous bcc solid solutions.⁶ We have tried to check if disorder entropy could stabilize them. In order to do that, we have crudely assumed that, for any given composition, all contributions to the entropy are the same for a definite compound and a disordered system, but for a disorder term:

$$\Delta S_{\text{mix}}^{\text{ideal}} = -R[x \ln x + (1-x)\ln(1-x)], \quad (11)$$

where R is the perfect gas constant and x the concentration. The term $-T\Delta S$ can be estimated to be 5.3 mRy per atom for a temperature of 1200 K and an equiatomic concentration ($x=0.5$).

Taking into account this effect on our DFT calculations indeed stabilizes the disordered solutions with respect to intermetallic compounds, at a temperature of 1200 K. This is represented on Fig. 6.

However, contrary to experiment, the asymmetry remains on the W-rich side of the graph.

IV. MELTING PROPERTIES

We then used our potential to calculate melting temperatures of Ta-W alloys. The melting temperatures T_m were calculated by a solid-liquid coexistence molecular dynamics method.^{31,32} In this technique, a starting sample is prepared at a given temperature, half solid and half liquid. The calcu-

TABLE V. Values of the angular screening parameters C_{\min} and C_{\max} for each interaction in Ta-W alloys.

	Ta-Ta-Ta	Ta-W-Ta	Ta-Ta-W	Ta-W-W	W-Ta-W	W-W-W
C_{\min}	0.25	0.30	0.22	0.37	0.19	0.49
C_{\max}	2.80	2.98	2.87	2.75	2.25	2.80

TABLE VI. Equilibrium lattice parameters and formation energies of various structures not included in the fit of the improved 2NN-MEAM potential. The definition of the $\text{Mo}_{1-x}\text{Ta}_x$ structures can be found in Ref. 3. Our *ab initio* results are also added.

Structure	x_W	<i>Ab initio</i>		2NN-MEAM	
		a_0	E^f	a_0	E^f
Ta_{12}W_4 (“ $\text{Mo}_4\text{Ta}_{12}$ ”)	0.25	3.275	-4.94	3.272	-3.31
Ta_9W_4 (“ Mo_4Ta_9 ”)	0.31	3.272	-3.21	3.271	-4.03
Ta_2W ($C11_b$)	0.33	3.259	-5.87	3.260	-4.56
Ta_3W_2 (“ Mo_3Ta_2 ”)	0.40	3.261	-6.45	3.260	-5.91
TaW ($B32$)	0.50	3.244	-5.46	3.249	-9.20
Ta_3W_4	0.57	3.255	-6.51	3.257	-5.28
Ta_2W_3 (“ Mo_3Ta_2 ”)	0.60	3.232	-8.98	3.234	-7.62
TaW_2 ($C11_b$)	0.67	3.220	-8.58	3.221	-7.68
TaW_5 (AB_5)	0.83	3.208	-5.26	3.209	-4.45

lations were performed in NVE ensemble, including steps for controlling temperature and pressure. The whole crystal is thermalized at a temperature T_0 which is assumed to be close to the melting temperature. Then the integration of the equations of motion is stopped in the solid part whereas temperature is increased, so as to melt the other part. Then the molten side is brought back to the temperature T_0 by rapid quenching. The equations of motion are then integrated for all the atoms, and the system is left free to evolve. The melting temperatures are determined by examining the evolution of the solid-liquid interface. When it is stable during this last simulation (at least for a few dozens of picoseconds) we reach a point in the melting curve.³⁷ Histograms of the atomic positions are recorded during the simulation: They enable us to accurately locate the solid/liquid interface versus time. We have performed molecular dynamics simulations using a box twice long as large. The number of atoms varied from 2048 ($16 \times 8 \times 8$) atoms for $B2$ structure and pure metals to 8788 ($26 \times 13 \times 13$) atoms for bcc solid solutions.

For the pure metals, the calculated melting temperatures are 3200 K for Ta and 4600 K, for W whereas the experi-

TABLE VII. Equilibrium lattice parameters and formation energies of Ta-W bcc solid solutions, obtained with the improved 2NN-MEAM potential. All atomic positions are relaxed.

x_W	a_0 (Å)	E^f (mRy/atom)
0.10	3.306	-1.17
0.20	3.291	-2.50
0.25	3.283	-3.19
0.30	3.276	-3.88
0.40	3.262	-5.11
0.50	3.249	-6.01
0.60	3.236	-6.50
0.70	3.224	-6.24
0.75	3.218	-5.83
0.80	3.212	-5.19
0.90	3.201	-3.22

mental values³³ are 3290 K, and 3695 K, respectively. We have estimated the corresponding heats of melting to be 22.0 and 34.0 kJ/mol for Ta and W. They clearly underestimate the experimental values which are respectively 36.6 and 52.3 kJ/mol according to Ref. 34. These discrepancies point out the difficulty of reproducing liquid properties with a potential parametrized on solid properties. To overcome this problem one should include physical characteristics of the liquid state in the potential-fitting procedure. As we will see in the following, we have tried instead to smooth the repulsive part of the W potential in order to reduce the predicted melting temperature since the purpose of this work was not to reparametrize potentials for pure Ta and W. Our results agree with MD results of Lee *et al.*⁴ which is not surprising since we are using 2NN-MEAM potentials based on the one they have published. As mentioned earlier, the melting temperature of the W potential is strikingly bad. In order to correct for that, we have tried to modify some of the parameters. One simple way to try, is to vary the d parameter in the Rose equation, in order to smooth the potential and to allow consequently the melting at a lower temperature. Thus, if one

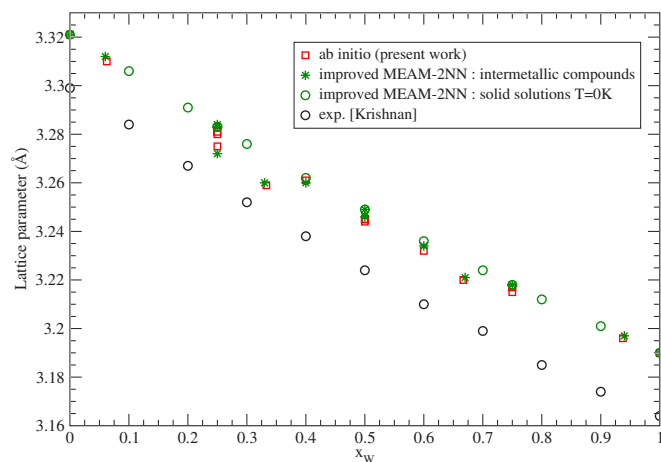


FIG. 5. (Color online) Equilibrium lattice parameters of Ta-W structures and bcc solid solutions as a function of W composition, predicted by the improved 2NN-MEAM potential.

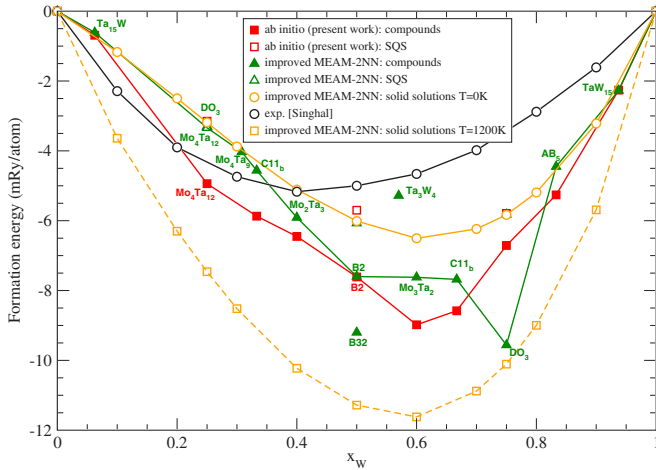


FIG. 6. (Color online) Formation energies of $Ta_{1-x}W_x$ structures and bcc solid solutions as a function of W composition, predicted by the improved 2NN-MEAM potential. The curve at $T=1200$ K accounts for an ideal mixing entropy.

chooses a value of -0.005 instead of 0.00 for d , T_m is reduced by 200 K. Nevertheless this reduction is small compared to the difference between predicted and experimental melting temperatures, around 1000 K.

A second method would require deeper modifications of the 2NN-MEAM potential. The angular screening defined by the parameters C_{\min} and C_{\max} should be modified. Consequently, to maintain a reasonable description of physical properties such as elastic constants, it would be necessary also to readjust the weights $t^{(l)}$. This procedure, whose result is not guaranteed, is beyond the scope of this paper.

So, given our potentials, the melting temperatures of five $Ta_{1-x}W_x$ intermetallic compounds and three Ta-W bcc solid solutions have been predicted. Their values are plotted on Fig. 7 as a function of W composition. If an ideal mixing law is assumed, the melting temperature of an $A_{1-x}B_x$ alloy at low concentrations can be estimated by the following formula:^{35,36}

$$T_m^{\text{alloy}}(x) = \frac{1}{\frac{1}{T_m} - \frac{k_b}{\Delta H_m} \ln(1-x)}, \quad (12)$$

where x is the composition of the impurity, k_b the Boltzmann constant, and ΔH_m and T_m the melting enthalpy and temperature of the pure metal A . This corresponds to the dashed lines on Fig. 7, respectively for the Ta and W potentials.

Our calculated melting temperatures are always higher than the ones predicted by this simple law. Due to the poor prediction of the melting temperature for pure W, we cannot

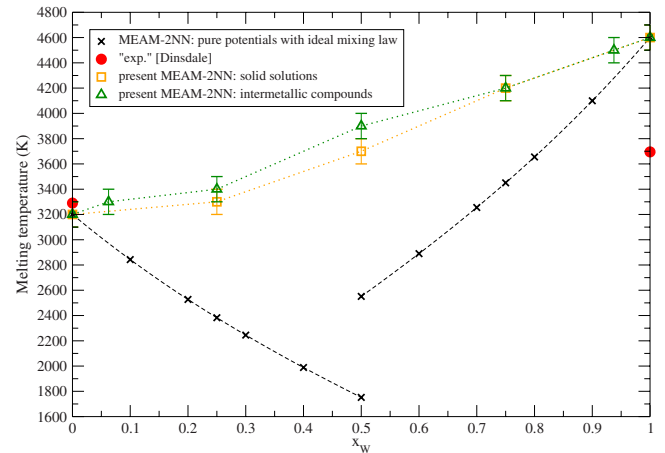


FIG. 7. (Color online) Melting temperatures of intermetallic compounds and bcc solid solutions of Ta-W alloys, as a function of W composition. Our results are obtained from molecular dynamics simulations using our improved 2NN-MEAM potential. Experimental data are from Ref. 33. Results with a 2NN-MEAM potential are estimated from an ideal mixing law [Eq. (12)].

draw ultimate conclusions. However, we think that, even with a better W potential, TaW systems would show a noticeable departure from an ideal mixing law.

V. CONCLUSION

We have presented in this paper a methodology which enabled us to build a fairly transferable 2NN-MEAM Ta-W cross potential from first-principles calculations. A first and straightforward attempt proved to be insufficient; we had to consider a more subtle screening to obtain a good transferability of the potential, whatever the composition of the alloy. This potential has been applied to the calculation of the melting temperatures of these alloys as a function of concentration. We think that this methodology can be applied to other metallic compounds. A better agreement with experiment would imply to develop a new 2NN-MEAM potential for W.

ACKNOWLEDGMENTS

We acknowledge Pierre-Matthieu Anglade for his help in the construction of the MEAM potential and in the development of the calculation of melting points. We acknowledge also M. I. Baskes for his advice in the way to improve a potential.

- ¹P. E. A. Turchi, A. Gonis, V. Drchal, and J. Kudrnovsky, Phys. Rev. B **64**, 085112 (2001).
- ²C. Jiang, C. Wolverton, J. Sofo, L-Q. Chen, and Z-K. Liu, Phys. Rev. B **69**, 214202 (2004).
- ³V. Blum and A. Zunger, Phys. Rev. B **72**, 020104(R) (2005).
- ⁴B.-J. Lee, M. I. Baskes, H. Kim, and Y. K. Cho, Phys. Rev. B **64**, 184102 (2001).
- ⁵R. Krishnan, S. P. Garg, and N. Krishnamurthy, J. Alloy Phase Diagrams **3**, 1 (1987).
- ⁶S. C. Singhal and W. L. Worrell, Metall. Trans. **4**, 895 (1973).
- ⁷V. Blum and A. Zunger, Phys. Rev. B **69**, 020103(R) (2004).
- ⁸V. Blum and A. Zunger, Phys. Rev. B **70**, 155108 (2004).
- ⁹P. Hohenberg and W. Kohn, Phys. Rev. **136**, B864 (1964).
- ¹⁰G. Kresse and J. Furthmüller, Comput. Mater. Sci. **6**, 15 (1996).
- ¹¹J. P. Perdew, J. A. Chevary, S. H. Vosko, K. A. Jackson, M. R. Pederson, D. J. Singh, and C. Fiolhais, Phys. Rev. B **46**, 6671 (1992).
- ¹²H. J. Monkhorst and J. D. Pack, Phys. Rev. B **13**, 5188 (1976).
- ¹³M. Methfessel and A. T. Paxton, Phys. Rev. B **40**, 3616 (1989).
- ¹⁴C. Bercegeay and S. Bernard, Phys. Rev. B **72**, 214101 (2005).
- ¹⁵M. S. Daw and M. I. Baskes, Phys. Rev. Lett. **50**, 1285 (1983).
- ¹⁶M. S. Daw and M. I. Baskes, Phys. Rev. B **29**, 6443 (1984).
- ¹⁷M. S. Daw, S. M. Foiles, and M. I. Baskes, Mater. Sci. Rep. **9**, 251 (1993).
- ¹⁸M. I. Baskes, J. S. Nelson, and A. F. Wright, Phys. Rev. B **40**, 6085 (1989).
- ¹⁹M. I. Baskes, Phys. Rev. B **46**, 2727 (1992).
- ²⁰M. I. Baskes, J. E. Angelo, and C. L. Bisson, Modell. Simul. Mater. Sci. Eng. **2**, 505 (1994).
- ²¹M. I. Baskes, Mater. Chem. Phys. **50**, 152 (1997).
- ²²B.-J. Lee and M. I. Baskes, Phys. Rev. B **62**, 8564 (2000).
- ²³M. I. Baskes, Phys. Rev. Lett. **59**, 2666 (1987).
- ²⁴J. E. Angelo, M. I. Baskes, and C. L. Bisson, Modell. Simul. Mater. Sci. Eng. **2**, 505 (1994).
- ²⁵M. I. Baskes, Mater. Sci. Eng., A **261**, 165 (1999).
- ²⁶J. H. Rose, J. R. Smith, F. Guinea, and J. Ferrante, Phys. Rev. B **29**, 2963 (1984).
- ²⁷B.-J. Lee, J.-H. Shim, and H. M. Park, CALPHAD: Comput. Coupling Phase Diagrams Thermochem. **25**, 527 (2001).
- ²⁸G. Marsaglia, Ann. Math. Stat. **43**, 645 (1972).
- ²⁹G. E. P. Box and M. E. Muller, Ann. Math. Stat. **29**, 610 (1958).
- ³⁰X. Ni, X. Wang, and G. Chen, Rare Metals **20**, 13 (2001).
- ³¹O. Tomagnini, F. Ercolessi, S. Iarlori, F. D. Di Tolla, and E. Tosatti, Phys. Rev. Lett. **76**, 1118 (1996).
- ³²A. Laio, S. Bernard, G. L. Chiarotti, S. Scandolo, and E. Tosatti, Science **287**, 1027 (2000).
- ³³A. T. Dinsdale, CALPHAD: Comput. Coupling Phase Diagrams Thermochem. **15**, 317 (1991).
- ³⁴*Smithells Metals Reference Book*, 7th ed., edited by E. A. Brandes and G. B. Brook (Butterworth-Heinemann, Oxford, 1992).
- ³⁵O. L. Anderson and A. Duba, J. Geophys. Res. **102**, 22659 (1997).
- ³⁶J.-P. Poirier, *Introduction to the Physics of the Earth's Interior* (Cambridge University Press, Cambridge, UK 1991), Chap. 5.
- ³⁷Obviously, it is quite difficult to be sure that the interface would not move if the simulation was carried on more longer. For this reason, we performed simulations increasing the temperature by steps of 100 K and we consider that the melting point is located in between the two simulations for which we observe crystallization and melting. The estimated error on the melting temperature is thus on the order of 100 K.